Published in final edited form as:
J Bodyw Mov Ther. 2010 April ; 14(2): 162–171. doi:10.1016/j.jbmt.2010.01.002.

In Vitro Modeling of Repetitive Motion Injury and Myofascial Release

Kate R. Meltzer, M.S[1], **Thanh V. Cao, B.A.**[1], **Joseph F. Schad, M.S.**[2], **Hollis King, D.O., PhD**[3], **Scott T. Stoll, D.O., PhD**[4], and **Paul R. Standley, Ph.D.**[1]

[1]Department of Basic Medical Sciences, University of Arizona-College of Medicine, Phoenix, AZ 85004

[2]Arizona College of Medicine, Midwestern University, Glendale, AZ 85308

[3]A.T. Still University, School of Osteopathic Medicine, Mesa, Arizona

[4]University of North Texas Health Sciences Center-Texas College of Osteopathic Medicine, Fort Worth, TX 76107

Abstract

Objective—In this study we modeled repetitive motion strain (RMS) and myofascial release (MFR) in vitro to investigate possible cellular and molecular mechanisms to potentially explain the immediate clinical outcomes associated with RMS and MFR.

Method—Cultured human fibroblasts were strained with 8 hours RMS, 60 seconds MFR and combined treatment; RMS+MFR. Fibroblasts were immediately sampled upon cessation of strain and evaluated for cell morphology, cytokine secretions, proliferation, apoptosis, and potential changes to intracellular signaling molecules.

Results—RMS induced fibroblast elongation of lameopodia, cellular decentralization, reduction of cell to cell contact and significant decreases in cell area to perimeter ratios compared to all other experimental groups ($p<0.0001$). Cellular proliferation indicated no change among any treatment group; however RMS resulted in a significant increase in apoptosis rate ($p<0.05$) along with increases in death-associated protein kinase (DAPK) and focal adhesion kinase (FAK) phosphorylation by 74% and 58% respectively, when compared to control. These responses were not observed in the MFR and RMS+MFR group. Of the twenty cytokines measured there was a significant increase in GRO secretion in the RMS+MFR group when compared to control and MFR alone.

Conclusion—Our modeled injury (RMS) appropriately displayed enhanced apoptosis activity and loss of intercellular integrity that is consistent with pro-apoptotic DAPK2 and FAK signaling. Treatment with MFR following RMS resulted in normalization in apoptotic rate and cell morphology both consistent with changes observed in DAPK2. These in vitro studies build upon the cellular evidence base needed to fully explain clinical efficacy of manual manipulative therapies.

Kindly address correspondence to: Paul R. Standley, Ph.D., Professor, University of Arizona, College of Medicine- Phoenix, ABC Building 1, Room 324, 425 N. 5th Street, Phoenix, AZ 85004-2157, Academic Office: 602-827-2107, Research Laboratory: 602-827-2132, Fax: 602-827-2127, standley@email.arizona.edu.

Keywords

Cyclic strain; Human fibroblasts; Morphology; myofascial release; repetitive motion strain

INTRODUCTION

Myofascial release (MFR) is a widely employed direct manual medicine treatment which utilizes specifically guided mechanical forces to manipulate and reduce myofascial restrictions of various somatic dysfunctions. MFR when used in conjunction with conventional treatment, is effective to provide immediate relief of pain and to reduce tissue tenderness (Hou et al 2002; Fernandez de las Penas et al 2005). Additional post-treatment clinical outcomes include attenuation of edema and inflammation, reduction of analgesic use, improved muscle recovery post trauma and increased range of motion in affected joints (Sucher 1993; Andersson et al 1999; Sucher et al 2005). Despite these reports for clinical efficacy, no cellular or molecular mechanisms conclusively have been shown to be responsible.

We previously reported that, in vitro, fibroblasts respond to repetitive mechanical strain with a delayed inflammatory response, upregulated nitric oxide secretions and increased cell proliferation (Dodd et al 2006; Eagan et al 2007; Meltzer and Standley 2007). This response was not observed in counterstrain treated fibroblasts. Importantly, RMS-induced inflammatory responses were attenuated by counterstrain (Meltzer and Standley 2007). Therefore, we focus here on the ability of fibroblasts to serve as a mechanotransducer by which they respond *acutely* to modeled repetitive motion strain (RMS) and modeled MFR. Specifically we will model repetitive motion strain and MFR in vitro by using human fibroblast tissue constructs and videomorphometric and palpometric data we have reported previously (Meltzer et al 2007). Similar to what we reported for counterstrain (Meltzer and Standley 2007), here we hypothesize that human fibroblasts secrete inflammatory mediators in response to RMS, and that modeled MFR reduces such secretions. Further, we hypothesize that RMS acutely induces fibroplasias (increased fibroblast hyperplasia and hypertrophy), while MFR acutely reverses this effects. Importantly since clinical reports suggest that *immediate* pain relief is attained post-MFR (Hou et al 2002; Fernandez de las Penas et al 2005), we will test the *immediate* effects of RMS and MFR strain paradigms on fibroblast cytokine secretion, morphology, proliferation and hypertrophy. This study will build upon cellular and molecular evidence to explain mechanisms underlying the immediate clinical outcomes associated with RMS and MFR.

Clinical Relevance of study

Under normal conditions the fascia moves with fluidity and is unrestricted to provide stability and structural support. However, the functional roles of the fascia may become impaired as a result of repetitive motion injury, physical trauma and inflammation. Traumatized fascia disrupts normal biomechanics of the body, increasing tension exerted on the system and causing myofascial pain and reduced range of motion. Myofascial release (MFR) is clinically effective to provide immediate pain relief and to improve physiologic functions that have been altered by somatic dysfunctions. Despite clinical efficacies, our understanding of the underlying mechanisms responsible is minimal. Here, we investigated the molecular and cellular effects of modeled repetitive motion strain (RMS) and MFR on human fibroblast constructs in vitro. Fibroblasts treated with modeled RMS responded with morphological changes as measured by cellular actin staining, reduction in area and perimeter ratios and increased focal adhesion kinase activity. Fibroblasts also displayed enhanced cellular apoptosis (programmed cell death), likely mediated by death-associated protein kinase. Fibroblasts strained by RMS followed by MFR displayed attenuation in these responses. Modification of these cellular

properties may predispose to myofascial restrictions and tension and alleviation of symptoms with MFR noted in vivo. While clinical MFR directs force to fascial fibroblasts, indirect strains applied to nerves, blood vessels, lymphatic system, and muscles were not considered in this model. Despite the limitations of this in vitro modeling, these and other data from our laboratory suggest that fibroblasts, the primary cell type of the fascia, adapt specifically to mechanical loading in manners dependant upon strain magnitude, duration and frequency. This cellular strain model may prove useful to further investigate mechanisms and to build a cellular evidence base describing the positive outcomes of applied manual treatments in the clinical setting.

Description of Clinical MFR Methodology

Several challenges exist in order to effectively model MFR in vitro including accurately modeling strain directions, durations, frequencies and magnitudes. In an attempt to improve our modeling techniques, we have analyzed digital video data of several osteopathic manual treatments (OMTs) performed by osteopathic clinicians. Figure 1 shows two still frames of a video segment illustrating the procedure used to analyze MFR strain direction, frequencies and durations. Figure 1A shows the neutral, pretreatment positioning of the patient and clinician's hands prior to MFR. A clear Plexiglas sheet was immobilized approximately 24 inches above the patient in a manner that did not interfere with MFR. On the sheet were placed a series of three black dots, representing the neutral position and two arrows representing the strain direction in which the treatment will be applied. On the patient, a series of three red dots were applied to indicate the change in position of the skin, relative to neutral pre-strain, when strain is applied. In this pretreatment frame, the dark and light dots are superimposed upon one another. In Figure 1B, the direct MFR is applied (in a manner with sufficient force to engage the deep fascia as determined by clinician palpation) as shown by displacement of the two series of dots. The displacement indicates superior, lateral, and clockwise strains imparted to the fascia and underlying muscle. Data from these frames and several additional MFR sessions were captured digitally (Scion Image software suite) to analyze the superior and lateral strain (by measuring the inter-dot distances in the superior/inferior and lateral/medial fields) and the clockwise rotational strain (i.e., torque; by measuring angle of deviation from the pre-treatment parallel relationship of the two series of dots)." From these data, we utilized the following to generate our in vitro strain profile: time to load, duration of static strain, and time to unload. Strain magnitude used in the current study was equivalent to those studied in published reports. Strain direction, although equiradial in the current study, often includes heterobiaxial, uniaxial and shear in clinical settings.

METHODS AND MATERIAL

Human Fibroblast Cultures

Normal human dermal fibroblasts (NHDF) from Cambrex Laboratories (East Rutherford, New Jersey) were used for all experiments. Cells were cultured in Fibroblast Basal Medium (FBM; Cambrex Laboratories) at 37°C, 5% CO_2, and 100% humidity. FBM was changed every other day and NHDF were passed at confluence (usually 7 to 14 days). Experiments utilized passage numbers 2 through 6.

In Vitro Strain Apparatus

The Flexercell FX-4000 Tension Plus System (Flexcell International Corp, Hillsborough, NC) is a computer-based system, which utilizes vacuum to strain cells adhered to flexible collagen-coated membranes arranged in a 6-well per plate format. The deformation of the collagen causes the attached fibroblasts to also deform. Strain profiles are created by programming the magnitude, duration, direction and frequency of the negative pressure to create the desired profile. We have reported utilizing this apparatus to effectively model aortic pressure

waveforms (Standley et al 1999; Standley et al 2001), injury (Meltzer and Standley 2007), and counterstrain (Eagan et al 2007; Meltzer and Standley 2007).

Strain Profiles

NHDF were seeded (120,000 cells / well) onto collagen I-coated Bioflex plates, six wells per treatment group. Once cells were approximately 50-60% confluent (approximately 24 hrs post seeding), FBM was replaced with a reduced-serum medium (0.2% FBS) to induce quiescence. After 24 hours, cells were subjected to mechanical strain profiles. Strain profiles were designed to simulate a repetitive motion injury (eight hours of RMS; Fig 2A) and a simulated myofascial release (60 seconds of MFR; Fig 2B) based upon videomorphometric analysis of clinical MFR treatments (Meltzer et al 2007). The following four strain regimens were tested:

1. **Control:** cells were not subjected to any strain protocol for the duration of the experiments.
2. **RMS** (Repetitive Motion Strain): cells were subjected to the RMS profile (Fig 2A) for 8 hours, and then sampled immediately upon cessation of RMS.
3. **MFR** (Myofascial Release): cells were subjected to the MFR profile (Fig 2B) for 60 seconds, and then sampled immediately upon cessation of MFR.
4. **RMS+MFR:** cells were subjected to the 8 hours RMS protocol followed three hours later by the 60 second MFR protocol and then sampled immediately after cessation of MFR.

Photomicrographs

Fibroblast tissue constructs were analyzed microscopically for potential differences in cell morphology including lamellopodia elongation and/or truncation, cell membrane blebbing and removal from the collagen matrix. NHDF were also immunohistochemically stained with rhodamine-tagged phalloiden and subsequently observed for potential actin microfilament reorganization. Photomicrographs of each treatment group were also analyzed for cell counts per high powered field (HPF), cell area and cell perimeter using Image J 1.40g (National Institute of Health, USA; http://rsb.info.nih.gov/ij/) and Prism 4.03 (GraphPad Software, Inc., San Diego, California).

Cell Viability and Growth Measurements

Cell viability was confirmed and proliferation was measured using the CellTiter 96® Aqueous One Solution cell proliferation assay (Promega Corp.; Madison, WI).

Apoptosis Measurements

Apoptosis was measured using ssDNA Apoptosis ELISA kit (Chemicon International; Billerica, MA) in which formamide is used to denature cellular DNA with subsequent assessment of chromatin changes specific to apoptotic (and not necrotic) cells. The detection of denatured DNA was accomplished by using a monoclonal antibody to single-stranded DNA.

Intracellular Signaling Measurements

Potential changes in intracellular signaling molecules were assessed pair-wise for selected treatment groups. Each treatment group was composed of one to two pooled 6-well plates. Cell lysates were obtained by treatment with ice-cold lysis buffer (5 ml lysis buffer, 15 μl pepstatin A, 1mg/ml DMSO, 25 mg of a protease inhibitor cocktail (Roche Molecular Biochemicals, Indianapolis, IN) and 0.77 mg DTT). Lysates were centrifuged at 15,000 rpm at 4° C for 30 minutes and the supernatant was aspirated and collected and frozen at −80° C. Samples were then sent on dry ice for microarray processing (Kinexus Bioinformatics Corporation,

Vancouver, B.C. Canada). Expression levels and phosphorylation states of cell signaling proteins were assessed in duplicate.

Cytokine Secretion Measurements

Cytokine secretion was measured by testing the conditioned media on a quantifiable cytokine microarray (RayBiotech, Inc., Norcross, GA). Briefly, glass slides impregnated with antibodies of 20 cytokines in 16 replicate microarrays were incubated with blocking buffer, a 6-sample standard curve cytokine cocktail and conditioned media samples obtained from the four strain groups described above. Slides were then incubated with a detection antibody cocktail (Alexa Fluor 555-conjugated streptavidin) and the signal was detected with an Agilent Scanner G2505B. Data were extracted from the image via GenePix Pro 4.0 (Molecular Devices, Sunnyvale, CA), and then further analyzed with Q-Analyzer v3.5 (RayBiotech, Inc., Norcross, GA;). All data were corrected for volume and cell number before statistical analyses.

Statistical Analysis

Two to four experiments (with two to four replicates each) were completed to obtain the proliferation, cell count, protein, DNA, apoptosis and cytokine data presented. NHDF area and perimeter measurements were derived from 42-48 random cells per experimental group. Intracellular protein measurements were derived from 6-12 pooled replicate wells and each array was completed in duplicate. Cytokine results were then evaluated by Grubbs' Test to determine significant outliers from data set and further analyzed by a two-way ANOVA Bonferroni post-test. Additionally, all data were analyzed with a one-way ANOVA with post hoc Tukey's Multiple Comparison tests using Microsoft Excel (Microsoft Corporation) and Prism 4.03 (GraphPad Software, Inc., San Diego, California). Group means were considered significantly different if $p<0.05$.

Results

RMS-induced morphologic changes appear mediated when followed three hours later by MFR

Eight hours of RMS caused elongate lamellopodia, cellular decentralization, larger intercellular distances and reduced cell-cell contact area when compared to all other groups (Fig 3). Sixty seconds of MFR did not appear to cause these morphologic changes. When RMS is followed three hours later by MFR, the degree of lamellopodia presence / elongation and cytoplasmic condensation was reduced while intercellular distances and cell-cell contact area were mostly restored.

RMS causes NHDF area and perimeter changes

NHDF from all three strain groups displayed significantly decreased cellular area when compared to control cells (one-way ANOVA $p<0.0001$; Tukey post-hoc; Fig 4, top). RMS caused a significant increase in cell perimeter compared to all other treatment groups (one-way ANOVA $p<0.0001$; Tukey post-hoc; Fig 3, middle), while MFR resulted in significantly reduced cell perimeters vs. control and RMS groups only. NHDF from the control group displayed significantly greater area to perimeter ratios than any other group, NHDF from the RMS group displayed significantly reduced area to perimeter ratios vs. any other group (One-way ANOVA $p<0.0001$; Tukey post-hoc; Fig 4, bottom).

Fibroblast proliferation does not appear to be strain regulated

Cellular proliferation – as measured by cells per high powered field, the calorimetric proliferation assay, and DNA content – did not differ significantly among any of the four treatment groups (Figs 5 and 6). Differences in protein concentration among RMS, MFR or

RMS+MFR were found to be insignificant. A ratio of protein to DNA (as a proxy of cell hypertrophy) also showed no significant differences among any treatment groups (Fig 6d).

RMS causes apoptosis in fibroblasts

Eight hours of RMS caused a significant increase in apoptosis compared to control, MFR and RMS+MFR (One-way ANVOA $p<0.05$; Tukey post-hoc; Fig 7). There were no significant differences in apoptosis rates among control, MFR and RMS+MFR groups.

Intracellular Signaling Protein Results Suggest Support for Morphologic and Apoptotic Changes

Over six hundred intracellular signaling proteins were identified and compared by microarrays among the four treatment groups. While many displayed significant differences among the strain groups (data not shown for brevity), we focused our analyses on those that might suggest potential mediators of the observed cell morphology and apoptosis differences (Table 1). Our intracellular signaling results in the RMS treatment group showed that tyrosine 576 phosphorylated focal adhesion kinase (FAK^{Y576}) is upregulated by 58% when compared to control nonstrained NHDF. We also observed a 55% upregulation of phosphorylated peptide in the RMS+MFR group compared to RMS alone while there was only a 23% increase in the MFR group compared to control (averaged data from duplicate microarray spot analyses of 6-12 pooled lysate samples each). Death associated protein kinase 2 (DAPK-2), a signaling protein that mediates apoptosis, is upregulated by 74% in the RMS group compared to control. The other two comparisons (MFR vs. Control and RMS vs. RMS+MFR) revealed downregulation in this pro-apoptotic peptide of 12% and 10%, respectively. Serine 133 phosphorylated cyclic AMP response element binding protein ($CREB^{S133}$) causes an upregulation in transcription of numerous genes (Shaywitz and Greenberg 1999). NHDF subjected to RMS displayed a 159% increase in this phosphorylated peptide when compared to control. NHDF strained with the MFR protocol displayed an increase of only 21% compared to control, and those treated with RMS+MFR displayed only a 6% upregulation compared to the RMS group.

Analysis of cytokine secretion

NHDF secretions of twenty human cytokines were assessed immediately after cessation of the four strain treatments (Table 2). Of the 20 cytokines measured, IL-6, IL-8, and VEGF were secreted from NHDF in concentrations in excess of 100 pg/mL and GRO and MCP-1 secretion was greater than 1000 pg/mL as measured in conditioned media. All other cytokines were measured to be minimal immediately after cessation of strain. There was a significant increase in GRO secretion in the RMS+MFR group when compared to control and MFR group. All other cytokine secretions measured were found to be non significant among the four treatment groups.

DISCUSSION

To our knowledge, this is the first study to model MFR in an in vitro human fibroblast culture. While reports have shown various repetitive strain-induced changes in fibroblast proliferation, growth factor secretions and cellular alignment, ours is the first to show that several morphological changes in fibroblasts seen post repetitive strain are reversed if followed by modeled MFR. The lack of RMS-induced proliferation seen in this study may be masked by DAPK-2 associated apoptosis, an effect not seen in MFR or RMS+MFR groups. While we observed no differences among a number of secreted inflammatory and growth promoting mediators with the strain paradigms tested, we can not rule out up- or downregulation of their receptors, intracellular effectors or expression / secretion differences in non-measured

mediators. This in vitro strain model may be useful to further explore key cellular mechanisms that may underlie positive outcome of clinical MFR.

Fascia is a tough connective tissue that contains elastic fibers and its elasticity contributes to its passive resistance to tensile forces. Under normal conditions the fascia tends to be fluid and move with minimal restrictions. However, injuries resulting from physical trauma, repetitive motion strain and inflammation can decrease fascia tissue length and elasticity resulting in fascial restriction. Physical strain has also been shown to influence the density of fibroblasts, connective tissue proteins such as collagen and fascial myofibroblasts which may be capable of active fascial contraction (Schleip et al 2006). Injuries, such as repetitive motion strain, result in abnormal changes to tissue texture affecting passive and active resistance to motion which in turn leads to compromised joint articulation, discomfort, pain and reduced range of motion. Improvement in these sign and symptoms are often seen post MFR treatment (Sucher 1993; Andersson et al 1999; Hou et al 2002; Fernandez de las Penas et al 2005; Sucher et al 2005).

In our in vitro RMS model, NHDF tissue constructs displayed fibrotic looking cells with elongate actin-containing lamellopodia and general decentralization which are apparent in the enclosed photomicrograph. Significant decreases in area to perimeter ratio confirmed that substantial morphologic changes occurred in the RMS group that is indicative of cell elongation, increased intercellular distances and decrease cell-cell attachment area. If similar tissue changes occur in vivo in response to RMS, these findings may be characteristics of abnormal tissue texture change which, in turn, may attribute to fascia restriction.

We have previously reported that *acyclic* strain causes morphological changes in fibroblasts (Dodd et al 2006; Eagan et al 2007) while others have found cyclic strain-induced reorientation of fibroblasts (Jungbauer et al 2008; Wen et al 2009). Studies of fibroblast morphologic changes due to *cyclic* strain are scarce. However, in other cell types, cyclic stretching induced morphologic changes of HUVEC cells from a normal polygonal shape to elongated spindle-like shapes (Naruse et al 1998) and cyclic stretching of vascular smooth muscle cells have been shown to cause a variety of phenotypic changes including causing cell elongation (Riha et al 2005). To our knowledge this is the first study to investigate fibroblast morphology changes that may be consistent with fascial restrictions evident after repetitive motion injuries.

In addition to observing morphological changes we investigated several intracellular proteins that may be involved in the morphologic responses seen in the RMS group. We report upregulation of Focal Adhesion Kinase (FAK) phosphorylation at Tyrosine 576 by 58% in the RMS group compared to the control group. Focal Adhesion Kinase (FAK) is an important mediator of actin-extracellular matrix interaction and cell motility (Calalb et al 1995; Schlaepfer et al 2004) and the phosphorylation of FAK at Tyrosine 576 maximizes FAK activation (Calalb et al 1995). Changes in physical morphology require modifications of cell extracellular matrix interactions and our result of increased FAK activity is consistent with our observed morphology changes allowing structural stabilization during actin-cytoskeleton remodeling. In a related study, cyclic strain has been found to increase FAK tyrosine phosphorylation from minutes to hours and decrease in time frames greater than 24 hours (Naruse et al 1998; Molina et al 2001; Wang et al 2001). We observe similar results and report immediate response changes in FAK tyrosine phosphorylation immediately upon cessation of an 8hr cyclic strain.

Another intracellular protein that was accessed was death associated protein kinase (DAPK). DAPK has been found to pre-apoptotically stabilize stress fibers, but not maintain focal adhesions in quiescent murine embryonic fibroblasts (Kuo et al 2003). DAPK also triggers uncoupling of the formation of stress fibers and focal adhesions, possibly predisposing cell to

apoptosis which is found to occur after this uncoupling effect (Kuo et al 2003). Specifically, DAPK-2 is involved in apoptotic signaling (Kawai et al 1999), and its regulation influences overall fibroblast growth rates and, consequently, fibroplasia and alterations in tissue texture. Compared to control, RMS strained cells had a significant 21% increase in apoptosis concomitant with an upregulation of DAPK2 by 74%. Cyclic strain has been found to cause increases in apoptosis in mesenchymal stem cells (Kearney et al 2008), vascular endothelial cells (Kou et al 2009), and periodontal ligament cells (Zhong et al 2008). Fibroblasts apoptosis in response to cyclic strain has been mixed with increases seen from minutes (Skutek et al 2003) to days (Barkhausen et al 2003), decreases (Danciu et al 2004) and no change (Persoon-Rothert et al 2002; Nishimura et al 2007). Thus, the rate of apoptosis appears to be highly dependant on sampling time. Barkhausen et al (Barkhausen et al 2003) found an upregulation of apoptosis after one day, consistent with our findings, however, after two days apoptosis decreased. Apoptotic response to strain may change over time as the cells adapt to modified environments as induced, for example, by additional injurious strains or by manually directed strain maneuvers such as MFR.

Furthermore, we also observed a 159% increase in CREB phosphorylation at Serine 133 in the RMS test group. CREB phosphorylation at serine 133 is essential for CREB-mediated transcription and studies have shown its involvement in key cellular processes that include proliferation, differentiation and adaptive response (Shaywitz and Greenberg 1999). Upregulation in gene transcription may be associated with apoptotic, morphologic genes or cell surface receptor protein increasing NHDF sensitivity to select cytokine and growth factors. For example, studies have shown that fibroblasts cyclically strained resulted in an increase in cell proliferation (Webb et al 2006; Eagan et al 2007) but here we report that there were no significant changes in cell proliferation among the test groups. Cell proliferation was accessed by cell count per high powered field and confirmed be quantifying dsDNA. In addition, we have also shown that RMS treated cells resulted in an increase in apoptotic signaling. Significant increases in apoptosis should result in a decrease in total cell number however, this was not the case. Together, these data suggest that proliferation may have increased but the increase in apoptosis may have masked the proliferation rate resulting in no net gains. These data suggest that RMS in our NHDF tissue constructs bears many resemblances to injurious strain profiles noted in vivo.

In clinical application, manual manipulative therapy is effective in immediate response changes in tissue texture and pain threshold with patients diagnosed with mechanical neck pain (Fernandez de las Penas et al 2005). In a related report, MFR -- when used with other treatment modalities -- showed immediate reduction in pain and improved range of motion in patients with cervical myofascial dysfunction (Hou et al 2002). Our in vitro RMS+MFR model incorporated a three hour delay in between treatment to reflect the delay associated with patient seeking treatment at times after initially sustaining an injury. Although this delay may contribute to cell recovery after RMS, clinically this delay might be insignificant. In vitro analysis of the NHDF immediate proliferative response to a modeled MFR after injury showed a significant reduction in cellular apoptosis accompanied with a 10% decrease in DAPK-2 activation. To maintain non-fluctuation in cell numbers, as we did not observe changes in net cell proliferation in comparison to other treatment groups, the decrease in apoptosis may be correlated with a reduction in proliferation rate, as opposed to RMS.

Morphological changes induced by RMS were not observed in the RMS+MFR group. These data are complemented by results indicating significant increases in area to perimeter ratio in RMS+MFR when compared to RMS alone. It is interesting to speculate that the change in morphology and increase in area to perimeter ratio could be a reflection of tissue texture changes and increase elasticity of the myofascial layer resulting in improved range of motion seen in clinical applications.

In this study we broadened the search of cytokines that may be involved in immediately post treatment changes. Of the twenty cytokines measured we only observed a significant increase in GRO secretion in the RMS+MFR group when compared to control and MFR. GRO has been classified as a neutrolphil chemotractant and although studies have shown that GRO is unresponsive to induce proliferation in fibroblasts there is evidence to support its effect on regulating fibroblast collagen expression (Unemori et al 1993). This suggests that GRO may play a potential role in fibroblast actin-extracellular matrix remodeling as observed here in this study. All other cytokines secretion investigated were found to be non significant, however, we did observe an increasing trend in IL-1α in the RMS group compared to control which is consistent with our previous report (Meltzer and Standley 2007). Interestingly, RMS induced IL-1α expression was attenuated with the addition of MFR following RMS. The morphologic and apoptotic changes observed here appears to be independent of the cytokines we examined. However, the possibility of mechanical strain altering NHDF sensitivity to select cytokines through upregulating surface cell protein receptors is plausible. A 24hr post treatment investigation of cytokines is out of the scope of this study; however it may elucidate delayed cytokines secretion in response to the stimuli. Future studies will examine delayed secretion of cytokines and the immediate mediators of the morphologic and apoptotic changes observed in this study. Clinically, temporal delays from hours to days in cytokine induction, inflammatory processes, and pain after a repetitive motion strain type injury or a soft tissue trauma are well documented (Smith et al 2000; MacIntyre et al 2001; Hildebrand et al 2005). However, in this study we focused only on potential mediators of cellular changes that take place immediately post treatments.

Acknowledgments

We thank Chris Gooden, Diana Petitti, Michael Hicks and Shande Chen for their technical assistance.

Funding sources and conflicts of interest

Funding for these studies came from the National Institute of Health – National Center for Complementary and Alternative Medicine, the American Osteopathic Association and the Arizona Biomedical Research Collaborative. No authors declare any conflict of interest, financial or otherwise.

REFERENCES

Andersson GB, Lucente T, Davis AM, Kappler RE, Lipton JA, Leurgans S. A comparison of osteopathic spinal manipulation with standard care for patients with low back pain. N Engl J Med 1999;341(19): 1426–31. [PubMed: 10547405]

Barkhausen T, van Griensven M, Zeichen J, Bosch U. Modulation of cell functions of human tendon fibroblasts by different repetitive cyclic mechanical stress patterns. Exp Toxicol Pathol 2003;55(2-3): 153–8. [PubMed: 14620536]

Calalb MB, Polte TR, Hanks SK. Tyrosine phosphorylation of focal adhesion kinase at sites in the catalytic domain regulates kinase activity: a role for Src family kinases. Mol Cell Biol 1995;15(2): 954–63. [PubMed: 7529876]

Danciu TE, Gagari E, Adam RM, Damoulis PD, Freeman MR. Mechanical strain delivers anti-apoptotic and proliferative signals to gingival fibroblasts. J Dent Res 2004;83(8):596–601. [PubMed: 15271966]

Dodd JG, Good MM, Nguyen TL, Grigg AI, Batia LM, Standley PR. In vitro biophysical strain model for understanding mechanisms of osteopathic manipulative treatment. J Am Osteopath Assoc 2006;106(3):157–66. [PubMed: 16585384]

Eagan TS, Meltzer KR, Standley PR. Importance of strain direction in regulating human fibroblast proliferation and cytokine secretion: a useful in vitro model for soft tissue injury and manual medicine treatments. J Manipulative Physiol Ther 2007;30(8):584–92. [PubMed: 17996550]

Fernandez de las Penas C, Alonso-Blanco C, Fernandez-Carnero J, Miangolarra-Page JC. The immediate effect of ischemic compression technique and transverse friction massage on tenderness of active and latent myofascial trigger points: a pilot study. J Bodywork Mov Ther 2005;9(4):298–309.

Hildebrand F, Pape HC, Krettek C. [The importance of cytokines in the posttraumatic inflammatory reaction]. Unfallchirurg 2005;108(10):793–4. 796–803. [PubMed: 16175346]

Hou CR, Tsai LC, Cheng KF, Chung KC, Hong CZ. Immediate effects of various physical therapeutic modalities on cervical myofascial pain and trigger-point sensitivity. Arch Phys Med Rehabil 2002;83 (10):1406–14. [PubMed: 12370877]

Jungbauer S, Gao H, Spatz JP, Kemkemer R. Two characteristic regimes in frequency-dependent dynamic reorientation of fibroblasts on cyclically stretched substrates. Biophys J 2008;95(7):3470–8. [PubMed: 18515393]

Kawai T, Nomura F, Hoshino K, Copeland NG, Gilbert DJ, Jenkins NA, Akira S. Death-associated protein kinase 2 is a new calcium/calmodulin-dependent protein kinase that signals apoptosis through its catalytic activity. Oncogene 1999;18(23):3471–80. [PubMed: 10376525]

Kearney EM, Prendergast PJ, Campbell VA. Mechanisms of strain-mediated mesenchymal stem cell apoptosis. J Biomech Eng 2008;130(6):061004. [PubMed: 19045533]

Kou B, Zhang J, Singer DR. Effects of cyclic strain on endothelial cell apoptosis and tubulogenesis are dependent on ROS production via NAD(P)H subunit p22phox. Microvasc Res 2009;77(2):125–33. [PubMed: 18801380]

Kuo JC, Lin JR, Staddon JM, Hosoya H, Chen RH. Uncoordinated regulation of stress fibers and focal adhesions by DAP kinase. J Cell Sci 2003;116(Pt 23):4777–90. [PubMed: 14600263]

MacIntyre DL, Sorichter S, Mair J, Berg A, McKenzie DC. Markers of inflammation and myofibrillar proteins following eccentric exercise in humans. Eur J Appl Physiol 2001;84(3):180–6. [PubMed: 11320633]

Meltzer, KR.; Schad, JF.; King, H.; Stoll, ST.; Standley, PR. In vitro Human Fibroblast Model of Repetitive Motion Strain (RMS) and Direct OMT (DOMT): Roles for Proliferation and Apoptosis; 51st Annual AOA Research Conference Abstracts; 2007; 2007. p. 327-364.

Meltzer KR, Standley PR. Modeled repetitive motion strain and indirect osteopathic manipulative techniques in regulation of human fibroblast proliferation and interleukin secretion. J Am Osteopath Assoc 2007;107(12):527–36. [PubMed: 18178762]

Molina T, Kabsch K, Alonso A, Kohl A, Komposch G, Tomakidi P. Topographic changes of focal adhesion components and modulation of p125FAK activation in stretched human periodontal ligament fibroblasts. J Dent Res 2001;80(11):1984–9. [PubMed: 11759007]

Naruse K, Yamada T, Sai XR, Hamaguchi M, Sokabe M. Pp125FAK is required for stretch dependent morphological response of endothelial cells. Oncogene 1998;17(4):455–63. [PubMed: 9696039]

Nishimura K, Blume P, Ohgi S, Sumpio BE. Effect of different frequencies of tensile strain on human dermal fibroblast proliferation and survival. Wound Repair Regen 2007;15(5):646–56. [PubMed: 17971010]

Persoon-Rothert M, van der Wees KG, van der Laarse A. Mechanical overload-induced apoptosis: a study in cultured neonatal ventricular myocytes and fibroblasts. Mol Cell Biochem 2002;241(1-2):115–24. [PubMed: 12482033]

Riha GM, Lin PH, Lumsden AB, Yao Q, Chen C. Roles of hemodynamic forces in vascular cell differentiation. Ann Biomed Eng 2005;33(6):772–9. [PubMed: 16078617]

Schlaepfer DD, Mitra SK, Ilic D. Control of motile and invasive cell phenotypes by focal adhesion kinase. Biochim Biophys Acta 2004;1692(2-3):77–102. [PubMed: 15246681]

Schleip R, Naylor IL, Ursu D, Melzer W, Zorn A, Wilke HJ, Lehmann-Horn F, Klingler W. Passive muscle stiffness may be influenced by active contractility of intramuscular connective tissue. Med Hypotheses 2006;66(1):66–71. [PubMed: 16209907]

Shaywitz AJ, Greenberg ME. CREB: a stimulus-induced transcription factor activated by a diverse array of extracellular signals. Annu Rev Biochem 1999;68:821–61. [PubMed: 10872467]

Skutek M, van Griensven M, Zeichen J, Brauer N, Bosch U. Cyclic mechanical stretching of human patellar tendon fibroblasts: activation of JNK and modulation of apoptosis. Knee Surg Sports Traumatol Arthrosc 2003;11(2):122–9. [PubMed: 12664206]

Smith LL, Anwar A, Fragen M, Rananto C, Johnson R, Holbert D. Cytokines and cell adhesion molecules associated with high-intensity eccentric exercise. Eur J Appl Physiol 2000;82(1-2):61–7. [PubMed: 10879444]

Standley PR, Obards TJ, Martina CL. Cyclic stretch regulates autocrine IGF-I in vascular smooth muscle cells: implications in vascular hyperplasia. Am J Physiol 1999;276(4 Pt 1):E697–705. [PubMed: 10198306]

Standley PR, Stanley MA, Senechal P. Activation of mitogenic and antimitogenic pathways in cyclically stretched arterial smooth muscle. Am J Physiol Endocrinol Metab 2001;281(6):E1165–71. [PubMed: 11701430]

Sucher BM. Myofascial release of carpal tunnel syndrome. J Am Osteopath Assoc 1993;93(1):92–4. 100–1. [PubMed: 8423131]

Sucher BM, Hinrichs RN, Welcher RL, Quiroz LD, St Laurent BF, Morrison BJ. Manipulative treatment of carpal tunnel syndrome: biomechanical and osteopathic intervention to increase the length of the transverse carpal ligament: part 2. Effect of sex differences and manipulative “priming”. J Am Osteopath Assoc 2005;105(3):135–43. [PubMed: 15863733]

Unemori EN, Amento EP, Bauer EA, Horuk R. Melanoma growth-stimulatory activity/GRO decreases collagen expression by human fibroblasts. Regulation by C-X-C but not C-C cytokines. J Biol Chem 1993;268(2):1338–42. [PubMed: 8419336]

Wang JG, Miyazu M, Matsushita E, Sokabe M, Naruse K. Uniaxial cyclic stretch induces focal adhesion kinase (FAK) tyrosine phosphorylation followed by mitogen-activated protein kinase (MAPK) activation. Biochem Biophys Res Commun 2001;288(2):356–61. [PubMed: 11606050]

Webb K, Hitchcock RW, Smeal RM, Li W, Gray SD, Tresco PA. Cyclic strain increases fibroblast proliferation, matrix accumulation, and elastic modulus of fibroblast-seeded polyurethane constructs. J Biomech 2006;39(6):1136–44. [PubMed: 16256125]

Wen H, Blume PA, Sumpio BE. Role of integrins and focal adhesion kinase in the orientation of dermal fibroblasts exposed to cyclic strain. Int Wound J 2009;6(2):149–58. [PubMed: 19432665]

Zhong W, Xu C, Zhang F, Jiang X, Zhang X, Ye D. Cyclic stretching force-induced early apoptosis in human periodontal ligament cells. Oral Dis 2008;14(3):270–6. [PubMed: 18208476]

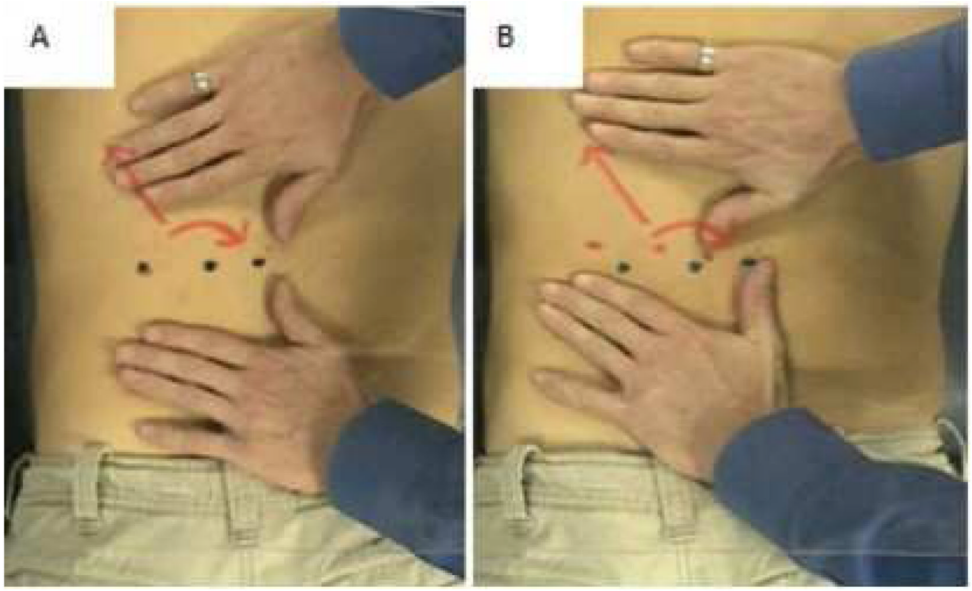

Figures 1.
AB. Still images captured from video clips of a clinical MFR treatment. (**A**) Clinician's hands and patient's back before treatment, and (**B**) the same placements during a 90 second MFR. Note the simultaneous superior, lateral and clockwise strain directions.

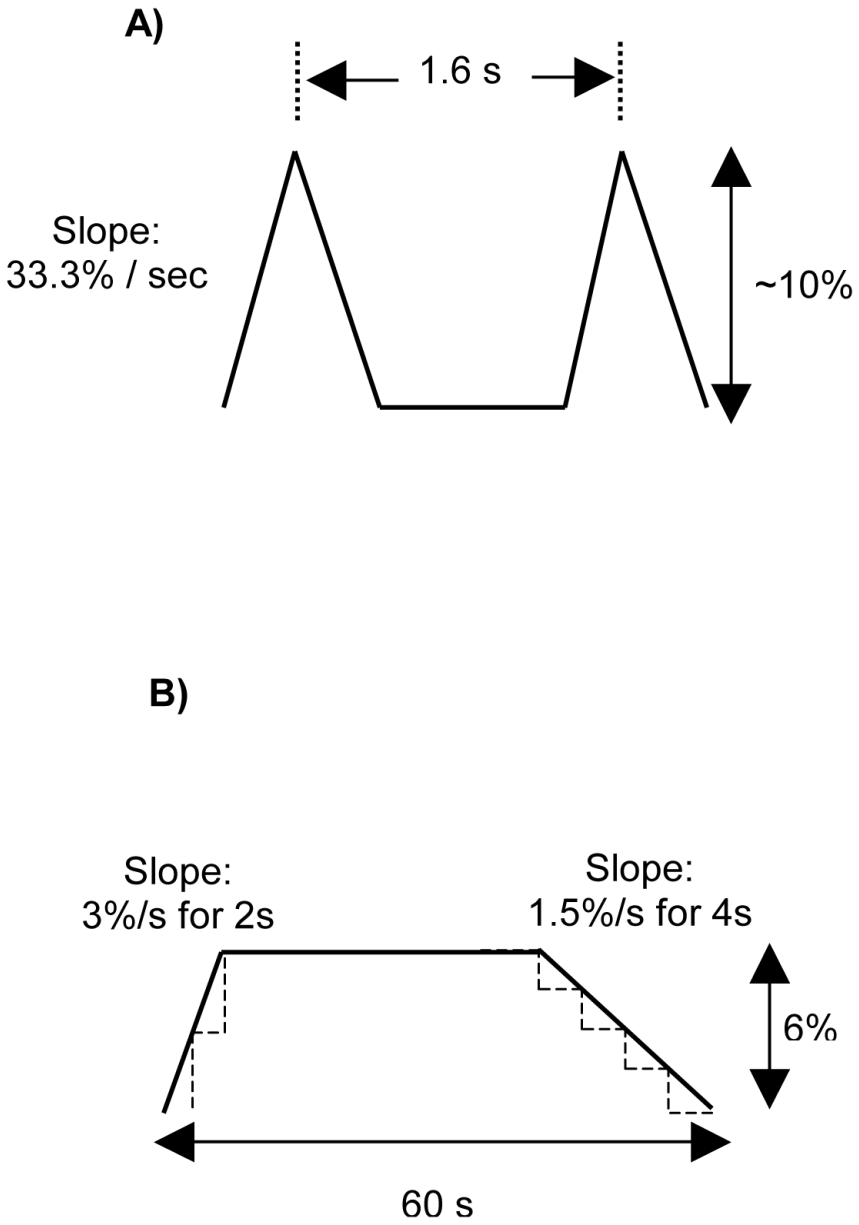

Figure 2.
Strain paradigm specifics for repetitive motion strain (RMS; A), and a complete 60 second cycle of modeled myofascial release (MFR; B).

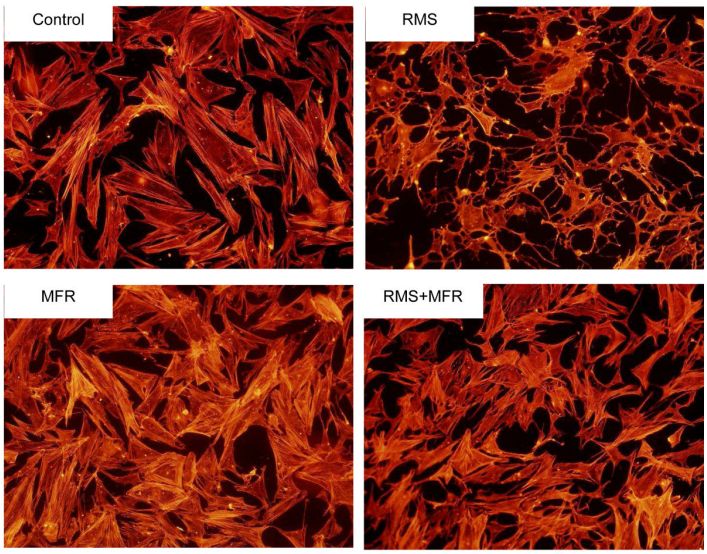

Figure 3.
Representative photomicrographs of human fibroblast construct morphology, growth patterns and actin architecture of the four treatment groups: Control, repetitive motion strain (RMS), myofascial release (MFR), and RMS+MFR.

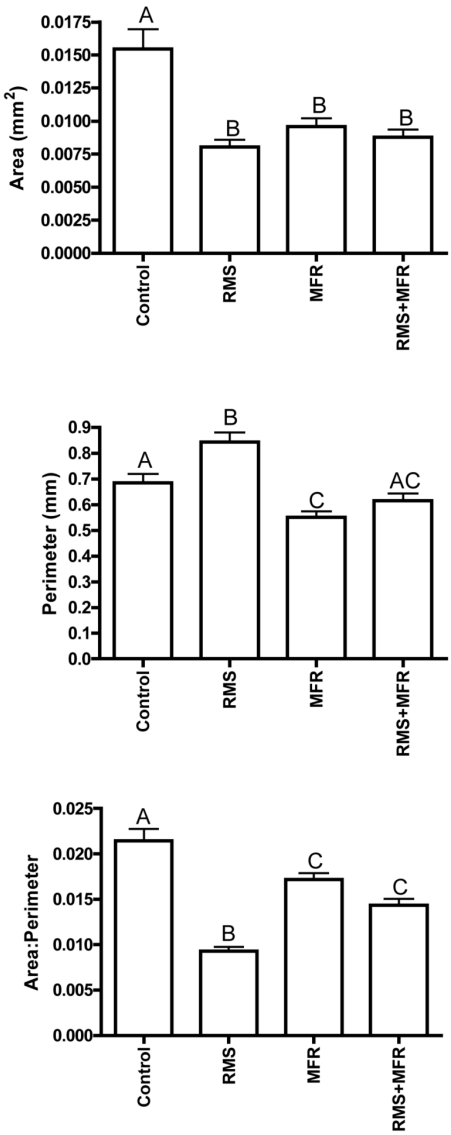

Figure 4.

Cell area (top), perimeter (middle) and area:perimeter (bottom) assessed from photomicrographs via digital image capturing. Different letters denote significant relationships among groups (one-way ANOVA with post hoc Tukey Multiple Comparisons Test; $p<0.05$; N=42 to 48 cells analyzed per treatment group.

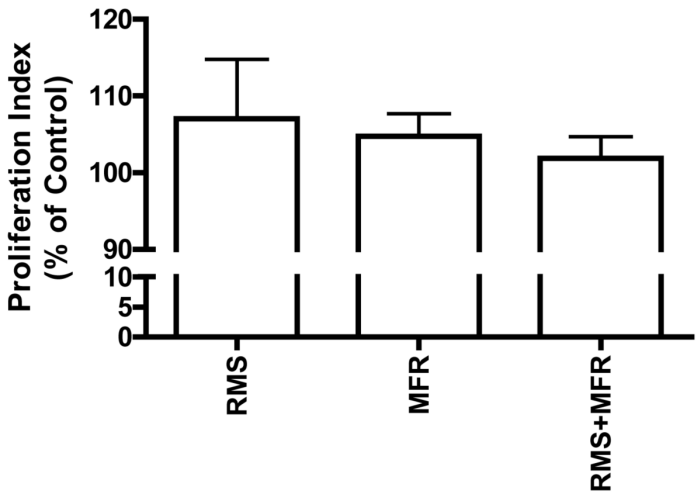

Figure 5.
Proliferation indicies, as measured calorimetrically with the CellTiter 96® Aqueous One Solution cell proliferation assay, of the treatment groups as a percent of non-strain control; N=3-4 ($p>0.05$).

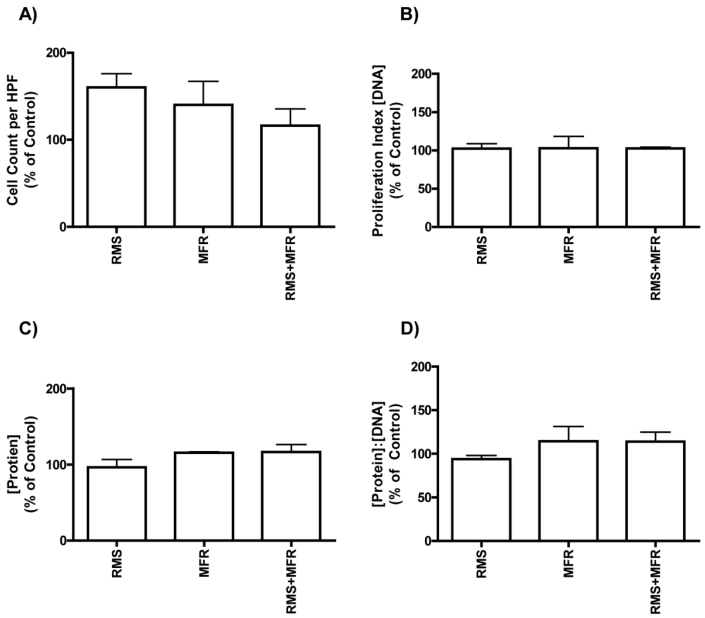

Figure 6.
Cell counts per high powered field (HPF; N=3 to 4 experiments), DNA, protein, and protein:DNA concentrations of treatment groups as a percent of control; N=2.

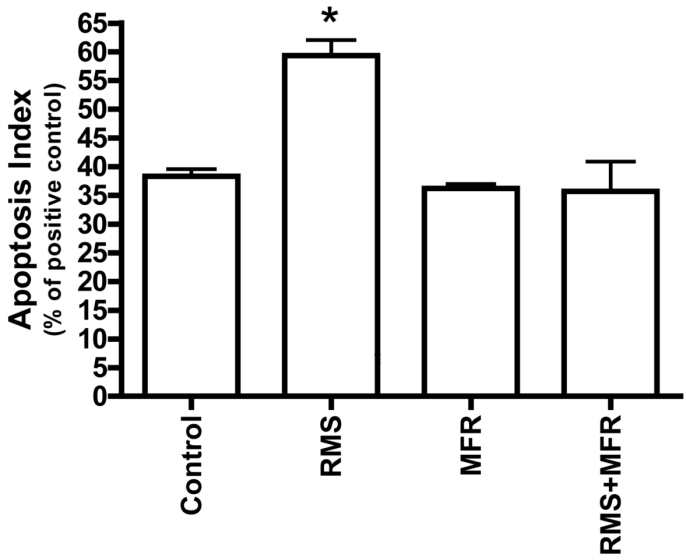

Figure 7.
Apoptosis indices of treatment groups as a percent of positive control. Significance determined via one-way ANOVA with post hoc Tukey Multiple Comparisons Test; $p<0.05$; N=2; *= significantly different from all other groups.

Table 1

Intracellular proteins of interest, their function, and percent change from control as assayed via Kinex™ Antibody Microarray

Protein or Phosphorylation Site	Function	Control vs. RMS	Control vs. MFR	RMS vs. RMS+MFR
DAPK-2	Positively mediates apoptosis	+74%	−12%	−10%
FAK^{Y576}	Maximizes FAK activation	+58%	+23%	+55%
CREB1^{S133}	Upregulates gene transcription	+159%	+21%	+6%

Table 2

NHDF secretion of select cytokines and growth factors from the four treatment groups described. Group means and SEMs are calculated with the exclusion of significant outliers determined by Grubbs' Test. All data are expressed in pg/ml (N=2-3)

	Treatment Groups							
	Control		RMS		MFR		RMS+MFR	
Cytokine	Mean	SEM	Mean	SEM	Mean	SEM	Mean	SEM
IL-1a	0.4	0.3	28.9	17.6	18.8	10.2	0.9	0.2
IL-1b	0.6	0.2	0.3	0.0	0.3	0.0	0.3	0.0
IL-2	5.4	0.4	5.0	0.1	5.2	0.5	5.4	0.4
IL-4	21.3	10.5	4.3	0.4	10.4	4.5	4.9	1.0
IL-5	0.4	0.0	0.4	0.0	0.5	0.1	2.2	1.0
IL-6	107.7	82.9	13.1	5.8	84.1	46.6	92.0	37.2
IL-8	146.4	1.5	226.3	71.6	91.4	5.9	123.7	34.2
IL-10	11.3	5.1	9.2	0.4	13.1	5.3	9.8	4.7
IL-12	6.6	3.9	5.8	0.1	0.7	0.1	13.6	0.1
IL-13	1.5	0.6	4.1	1.5	4.6	2.2	5.3	1.5
GM-CSF	0.4	0.0	1.3	0.5	0.3	0.1	0.4	0.0
GRO	1897.0	297.9	2595.0	921.5	1152.0	127.8	3761.0*	2037.0
IFNg	11.3	9.5	27.2	13.6	13.6	5.9	59.53	12.6
MCP-1	1467.0	551.0	1509.0	617.7	2225.0	952.0	2313.0	566.4
MIP-1a	8.3	4.7	11.6	5.4	5.3	1.7	10.8	4.1
MIP-1b	1.6	1.0	2.8	2.0	3.8	1.5	1.7	0.7
MMP-9	3.2	0.1	3.2	0.1	3.0	0.1	3.2	0.1
RANTES	10.9	7.3	2.2	0.7	13.2	8.3	2.0	1.0
TNFa	7.2	1.1	7.3	1.1	7.3	1.8	133.5	59.5
VEGF	256.9	44.3	275.2	14.4	800.9	126.3	493.5	129.0

* indicates significant differences compared to control and MFR